Title
Flame Surface Density and Burning Rate in Premixed Turbulent Flames

Author
Shepherd, I.G.

Publication Date
1995-10-01

LBL-37834
UC-400

Lawrence Berkeley Laboratory
UNIVERSITY OF CALIFORNIA

ENERGY & ENVIRONMENT DIVISION

Presented at the Fall Western States Section of the Combustion Institute; Stanford, CA; October 30-31, 1995 and to be published in the Proceedings

Flame Surface Density and Burning Rate in Premixed Turbulent Flames

I.G. Shepherd

October 1995

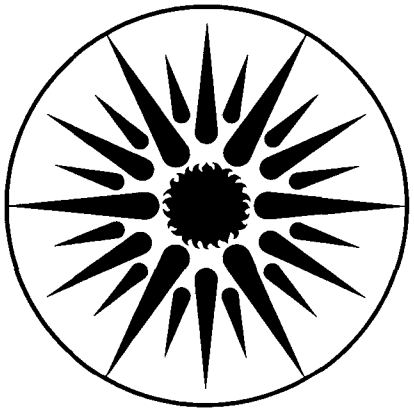

ENERGY AND ENVIRONMENT DIVISION

Prepared for the U.S. Department of Energy under Contract Number DE-AC03-76SF00098

DISCLAIMER

LBL-37834
UC-400

Flame Surface Density and Burning Rate in Premixed Turbulent Flames

I.G. Shepherd

Energy and Environment Division
Lawrence Berkeley National Laboratory
University of California
Berkeley, California 94720

October 1995

This work was supported by the Director, Office of Energy Research, Office of Basic Energy Sciences, Chemical Sciences Division of the U.S. Department of Energy under Contract No. DE-AC03-76SF00098

Flame Surface Density and Burning Rate in Premixed Turbulent Flames

I. G. Shepherd

Combustion Group, Energy and Environment Division
Lawrence Berkeley Laboratory
Berkeley, California 94720 USA

Abstract

The flame surface density has been measured in hydrocarbon/air stagnation point and v-shaped premixed turbulent flames. A method is proposed to determine the flame surface density from the data obtained by laser sheet tomography. The average flame length and flame zone area as a function of the progress variable are calculated from a map of progress variable and a set of flame edges obtained from the tomographs. From these results a surface density estimate in two dimensions is determined. By this technique it is possible to avoid the difficulties which arise when using an algebraic model based on the measurement of the flame front geometry and a scalar length scale. From these results the burning rate can be obtained which compares well with estimates calculated using the fractal technique. The present method, however, is not constrained by a minimum window size as is the case for the fractal determinations.

Introduction:

Two problems of great practical importance have dominated the study of premixed turbulent flames: the determination of the burning rate and, more recently, the measurement and understanding of pollutant formation. By analogy to laminar flames, where a burning velocity can be defined as a fundamental property of the system, in turbulent flames a turbulent burning velocity has been used to quantify the burning rate. A large amount of data has been accumulated [1] in an effort to relate the turbulent burning velocity to the characteristics of the turbulent field. Whether it is possible to reduce the complexities of these flames to such a parameter is still a moot point and recent work [2] has shown that many problems arise in the application of the burning velocity concept to practical flames.

An alternative approach to determining the burning rate has been to investigate the scalar field in premixed turbulent flame zones. Most of this work derives ultimately from the seminal insight of Damköhler who suggested that when the smallest turbulent scale is larger than the flame thickness the turbulent flow field will wrinkle the laminar flame front and so, by increasing its surface area, increase the burning rate. This, therefore, becomes the product of the flame surface area and S_L, the laminar burning velocity. This idea has found a wide range of application and has been formalized in terms of the flamelet concept [3]. Under this description a turbulent flame zone is viewed as an ensemble of laminar flamlets whose local burning rates are determined by the local flame stretch (the local flow strain, tangential to the flame surface, and local flame front curvature). The total burning rate of the flame is then the integration of the local burning rate over the flame surface. Bray [4] has given a simple expression for the burning rate at a point in a turbulent flame zone, w, which encapsulates these two factors:

$$\overline{w} = \rho_u S_L I_o \Sigma \qquad 1$$

where ρ_u is the unburnt gas density, I_o the mean modification to S_L arising from the local flame stretch and Σ is the local flame surface to volume ratio. The analysis of premixed turbulent flame can, therefore, be divided into two parts: the local burning rate and the area density of the front. It is the latter quantity that is the concern of this paper.

Under conditions of low to moderate turbulence when $I_o \sim 1$ the total burning rate, W is given by:

$$\overline{W} = \int_{z_u}^{z_b} \Sigma dz \qquad 2$$

where z is a coordinate which passes through the flame zone. A variety of methods have been used for determining Σ including algebraic [4], spectral [5] and fractal [6] techniques.

As part of a model of premixed turbulent combustion, Bray [4] has used algebraic expressions for Σ in terms of a progress variable, c, which is zero in the reactants and unity in the products:

$$\Sigma = \frac{g\bar{c}(1-\bar{c})}{\hat{L}_y}\left\langle\left|\frac{1}{\sigma}\right|\right\rangle \qquad 3$$

In this equation the term $\bar{c}(1-\bar{c})$, which is equal to c'^2, may be thought of as the probability of encountering a flame front at some point within the flame zone and it is scaled by the scalar integral length scale measured along the local $\bar{c}$ contour, $\hat{L}_y$. Although this is a one-dimensional formulation, account is taken of the flame orientation by the inclusion of the mean direction cosine between the flame front normal and the local $\bar{c}$ contour, σ. The development of laser tomography has made it possible to investigate this expression and studies of various flame configurations have been performed [7,8]. A problem, however, can arise in the determination of $\langle 1/\sigma \rangle$ from the experimental results. There is a finite probability that the flame front and local $\bar{c}$ contour become co-linear to give $\sigma=0$ and so generateing a singularity in $\langle 1/\sigma \rangle$.

In this paper the distribution of flame orientation in v-shaped and stagnation point premixed turbulent flames will be investigated and an alternative method for the determination of Σ in 2-dimensions will be described.

Experimental Details:

The experimental data was obtained from tomographic studies of a range of lean, hydrocarbon/air, stagnation-point, and a stoichiometric premixed turbulent flames. The Damköhler number at the cold boundary is large (~80) indicating that the flame is in the wrinkled laminar flame regime. The position of the flame front is determined from the intensity of light scattered from micron sized oil droplets seeded in the reactant stream which evaporate at the flame front. The oil droplets are illuminated by a laser sheet and photographed in a direction normal to the sheet.

An axisymmetric flow of premixed fuel and air at an exit velocity of *5m/s* is provided by a *50mm* diameter nozzle. A co-flowing air stream at the same velocity shields the inner flow from interaction with the room air. The reactant flow turbulence, generated by a perforated plate placed *50mm* upstream of the burner nozzle, has an integral length scale of *3mm* and the turbulent Reynolds number at the cold boundary is ~60. A stagnation plate is positioned *100mm* downstream of the nozzle exit. The burner configuration has been described in detail elsewhere[9]. Five flames are studied here: a methane/air flame (S1, ϕ=1.0) and three ethylene/air flames (S9, S10 and S11 with ϕ=1.0, 0.85, 0.75 respectively). The flow geometry chosen for this study has significant advantages in that the tomographic cross sections through the stagnation line provide a good statistical representation of the scalar field due to the axisymmetry of the system. For the v-shaped flame (a stoichiometric methane/air flame) a 2 mm rod, placed at the nozzle exit, is used as the flame holder and tomographic cross-sections through the flame zone normal to the center of the rod were taken.

A copper vapor laser producing *5mJ* pulses with a 20-30*nsecs* pulse width at *4kHz* allows resolution of the instantaneous flame shape. The laser sheet, *0.6mm* thick by *50mm* high with a field of view of *60mm*, is recorded by a *16mm* Fastax camera which provides the trigger pulse for the laser. The film is digitized with horizontal and vertical resolutions of 0.155 and 0.121 *mm*/pixel, respectively. The flame front is

clearly delineated as the interface between the light (cold reactants with seed particles) and dark (hot products without particles) regions of the image. Using an edge finding algorithm a continuous flame edge is obtained from each of the images. Each data set includes a least 200 images and each image has 512 by 512 pixels.

Results and Discussion:

Lee et al. [10] have investigated flame front orientation in a premixed turbulent flames and studied the evolution of its distribution with increasing u'/S_L. Given the transient nature of their experiment, however, they could not associate the orientations which were measured with a local $\bar{c}$ contour and so provided no information on the direction cosine which appears in equation 3.

This direction cosine at some point on the flame front is formed by the angle between the local $\bar{c}$ contour passing through it and the local normal to the flame front at that point. To obtain its distribution as a function of local $\bar{c}$ obtain it is necessary, therefore, to determine at each point on the flame fronts a) the $\bar{c}$ value, b) $\theta(x,y)$ where θ is the orientation of the $\bar{c}$ contour in laboratory coordinates (x,y) and c) $\phi(x,y)$ where ϕ is the tangent to the flame in laboratory coordinates.

$\theta(x,y)$ is obtained from a $\bar{c}$ map which is generated by the summation of binary images obtained by processing the each flame edge so that the burnt gas is given a value of 1 and the unburnt gas 0. An example of such a map for one side of the v-shaped flame is given in figure 1. Contours of constant $\bar{c}$ are now extracted by the thresholding and edge-finding technique outlined above. Ten evenly-spaced contours from $\bar{c}$ =0.05 to $\bar{c}$ =0.95 were obtained and by fitting and interpolation θ can be determined at any point in the $\bar{c}$ field.

A flame edge is then superimposed on the $\overline{C}$ map and for each point on the edge $\bar{c}$, θ and ϕ were calculated and a joint pdf , $P(\bar{c},\psi)$ was obtained for each case, where $\psi = \phi - \theta$. The tangent to the flame was obtained from 2nd order parametric fits through (x,s) and (y,s) for seven edge points around the point under consideration where s is the distance along the flame edge. Figure 2 shows the distribution of flame orientations, ψ, over the entire $\bar{c}$ space for case S1 and is typical of all the stagnation point flames. Inspection of the joint probability function, $P(\bar{c},\psi)$, shows that $\overline{\psi}$ is in the range $\pm 2^{o}$. ψ_{rms} increases with $\overline{C}$, figure 3, indicating that the flame orientation becomes more chaotic on the product side of the flame.

The distribution for the v-shaped flame, figure 4, shows a marked bimodality which becomes more pronounced as $\bar{c}$ increases. Such an evolution is consistent with the cusping of the flame front observed in these flames.

It will be noted that when ψ=0 then σ=0 and singularies will appear in the pdf of $1/\sigma$. Inspection of figures 2 and 4 show, therefore, that equation 3 cannot be used to determine the flame surface density in these flames.

Determination of Σ:

From the present data, however, it is possible to obtain a two dimensional estimate of Σ by a direct measurement of the flame length and the flame zone area as a function of the progress variable.

The flame zone area, $A(\bar{c})$, may be straightforwardly determined from the $\bar{c}$ map that was used in the previous section, figure 1. From the histogram of $\bar{c}$ values and a knowledge of the area of each pixel (0.155*0.121 mm) the flame zone area as a function of progress variable may be calculated: figure 5 shows these data for case S1. As might be expected the area has a maximum at the center of the flame zone where the $\bar{c}$ gradient is steepest and becomes very large as $\bar{c} \rightarrow 0,1$.

The length of the flame as a function of $\bar{c}$, $L(\bar{c})$, may be obtained in a similar manner. Each flame edge is smoothed by simple averaging to remove digitization noise and then, by interpolation, is divided into segments of equal length (0.1 mm). From the $\bar{c}$ map each segment is assigned a $\bar{c}$ value and the flame lengths are accumulated to give a total flame length, $L(\bar{c})$ for each complete data set. Figure 6 presents the average $L(\bar{c})$ for case S1; both this and figure 5 are typical of these results for the stagnation point and v-shaped flames. It is of interest to note that the flame length increases with the progress variable which is consistent with the geometry of these flames which are cusped towards the products, $\bar{c} \rightarrow 1$.

A two dimensional estimate for Σ, the length/area, may be readily calculated from this data:

$$\Sigma(\bar{c}) = \frac{L(\bar{c})}{A(\bar{c})} \qquad 4$$

Shown in figure 7 are the flame surface density results for all the stagnation point flames. The data has been normalized by the number of flame edges averaged. The solid line in figure 7 is $k\,\bar{c}\,(1-\bar{c})$ which may be compared to equation 2 where k (0.57 in this case) is a constant obtained from a least squares best fit of this expression through all the data. On comparison with equation 2 it will be seen that k has units of inverse length. This provides a good estimate of the experimental results where the increase in flame length observed in figure 6 is compensated, in part, by the asymmetry in the area function shown in figure 5. This characteristic variation of $\Sigma(\bar{c})$ has been observed in a range of flame configurations from a variety of temporal and spatial measurements [4].

Similar trends are observed for the v-shaped flame. Figure 8 shows the $\bar{c}$ contours derived from one half of the v-shaped flame $\bar{c}$ map. The contours diverge with increasing downstream distance and so the flame was divided into 10 mm sections spaced by 5 mm to investigate the spatial evolution of Σ. The sections were oriented so as to be normal to the $\bar{c}=0.5$ contour line. $\Sigma(\bar{c})$ results for the v-shaped flame are given in figure 9. These plots are significantly more asymmetric that those for the stagnation flame and so $k\,\bar{c}\,(1-\bar{c})$ will not provide as good an estimate for $\Sigma(\bar{c})$. Fits of this function to the data, however, show k to be falling with increasing downstream distance (see Table 2). The bimodal pdfs of flame orientation, figure 4, indicate a more ordered, cusped structure in the v-shaped flame and this probably contributes to the asymmetry observed in in figure 9.

Estimate of Burning Rate, $\overline{W}$

As indicated by equations 1,2 the burning rate when $I_o \sim 0$ can be obtained by the integration of the flame surface density through the flame zone. The integration path, z (z=0 at the center of the flame zone), for these planar flames will be normal to the $\bar{c}$ contours. In the v-shaped flame the divergence of the contours, figure 8, is small enough for the 10 mm normal segments to be considered planar without significant error. The transformation, $\bar{c}(z)$, is then the profile through $\bar{c}$ space, the average of which, due to the planar mean geometry, can be calculated from the cumulative distribution form of the histogram of the flame zone area, divided by the flame zone width. A continuous function for the transformation of this profile was obtained by fitting it with an expression derived from the KPP equation [11]:

$$\bar{c} = \frac{1}{1+\exp(-4z/\delta_T)} \qquad 5$$

where δ_T, the fitting parameter, is the flame zone thickness defined by the maximum $\bar{c}$ gradient. The progress variable in figure 7 can now be transformed into physical space by use of the inverse of equation 5, non-dimensionalized by the flame thickness, to give figure 10 for the stagnation flames. The solid line in the figure is $k\,\bar{c}\,(1-\bar{c})$ using the mean value of k determined above. The results shown in figure 10 indicate that in these flames a good estimate of the burning rate may be obtained from an integration of $k\,\bar{c}\,(1-\bar{c})$:

$$\overline{W} = k\int_{-\infty}^{\infty}\bar{c}(1-\bar{c})\,dz \qquad 6$$

Substituting for $\bar{c}$ in equation 6 and integrating gives

$$\overline{W} = \frac{k\,\delta_T}{4} \qquad 7$$

Shown in Table 1 are the burning rates of the stagnation point flames using equation 7. The k values are obtained from fitting the data shown in figure 7 for each case and the turbulent zone thickness is derived from the flame area data, figure 5, by the method outlined above. These results are compared in Table 1 with the burning rate calculated by the fractal technique[6], $\overline{W}_f$, and can be seen to be very similar. It should be noted that equation 7 indicates that a simple method of estimating the burning rate is now available. The constant k/4 in the equation is $k\,\bar{c}\,(1-\bar{c})$ at $\bar{c}=0.5$, figure 7, and so in these flames the burning rate can be estimated from the maximum of Σ:

$$\overline{W} \sim \delta_T \Sigma_{max} \qquad 8$$

Similar results have been obtained for the v-shaped flame, Table 2, although as pointed out above the fit here for equation 6 is less good. In this case an advantage over the fractal method becomes apparent. The flame thickness and burning rate increases with downstream distance, figure 8 and Table 2. The fractal method can only provide an average value (1.61) because the window for the calculation must be larger than the outer cutoff, ~ 19 mm, for a fractal estimate to be obtained

Conclusions:

A method has been proposed to determine the flame surface density in stagnation point and v-shaped premixed turbulent flames from the data obtained from laser sheet tomography. From a direct determination of the average flame length and flame zone area as a function of the progress variable and an estimate of theflame surface density in two dimensions can be obtained. It is then possible to avoid the difficulties which arise when using an algebraic model based on the measurement of the flame front geometry and a scalar length scale.

From these results the burning rate can be obtained which compares well with estimates calculated using the fractal technique. The present method, however, is not constrained by a minimum window size as is the case for the fractal determinations.

Acknowledgments:

This work was supported by the Director, Office of Energy Research, Office of Basic Energy Sciences, Chemical Sciences Division of the U.S. Department of Energy under contract No. DE-AC-03-76SF00098. The author is grateful to G. Hubbard for some of the data reduction software and discussions with K.N.C. Bray and Wm.T.Ashurst.

References:

1. Bradley,D., *Combustion & Flame*, 1995, **100**, p749.

2. Shepherd,I.G. and Kostiuk, L.W., *Combustion & Flame,* 1994, **96**, 371-380

3. Clavin, P., *Progress in Energy and Combustion Sciences*, 1985, **11**, 1.

4. Bray, K.N.C., *Proc. Roy. Soc.A,* 1990,**431**, 313-335.

5. Peters, N., *Journal of Fluid Mechanics*, 1992, **242**, 611-629.

6. Gouldin,F.C., Bray, K.N.C. and Chen,J.Y., *Combustion & Flame,* 1989, 77,241-259

7. Shepherd, I.G. and Ashurst, Wm.T., *24th Symposium (International) on Combustion*, 1992, 485-491.

8. Chew, T.C., Bray, K.N.C. and Britter, R.E., *Combustion and Flame*, 1991, **80**, 65-82.

9. Shepherd, I.G., Cheng,R.K., and Goix, P.J., *23rd Symposium (International) on Combustion*, 1990.

10. Lee, T.W., North, G.L. and Santavicca, D.A., *Combustion Science and Technology*, 1992, **84**, 121-132

11. Ashurst, Wm.T. and Shepherd, I.G., *Fall Meeting of the Western States Section of The Combustion Institute*, 1995.

	k (1/mm)	δ_T (mm)	k δ_T/4	$\overline{W}_f$
S1	0.571	10.5	1.50	1.48
S9	0.554	12.1	1.68	1.64
S10	0.563	9.8	1.38	1.46
S11	0.588	9.4	1.38	1.41

Table 1: Stagnation point flames

Distance from rod mm	k 1/mm	δ_T mm	$\overline{W}$
25	0.779	8.21	1.59
30	0.731	8.89	1.62
35	0.699	9.28	1.62
40	0.698	9.52	1.66
45	0.667	10.29	1.71

Table 2: V-shaped flames

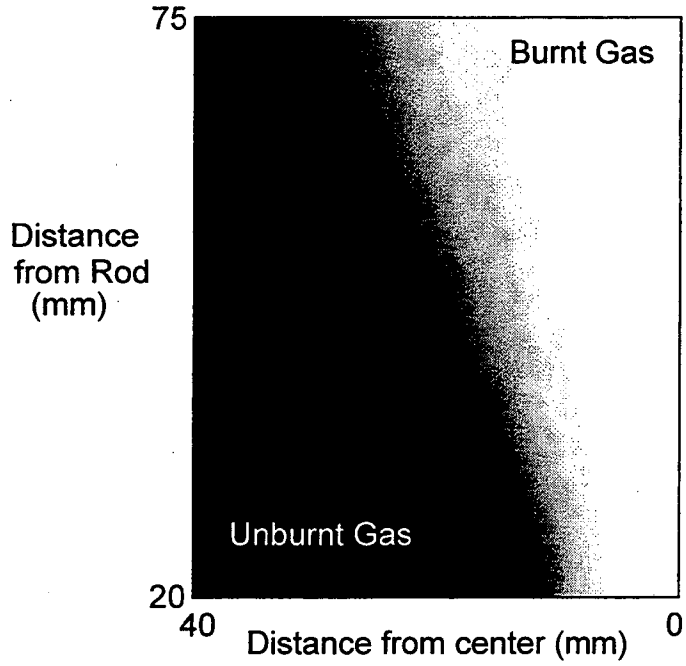

Figure 1 A $\overline{c}$ map for the stoichiometric methane/air v-shaped flame.

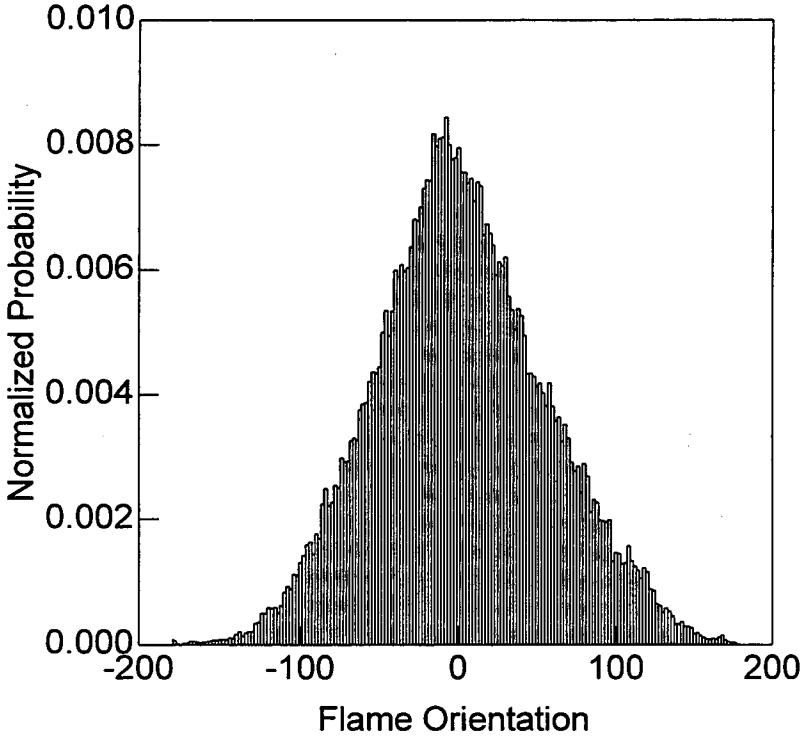

Figure 2 Probability distribution of flame orientation, ($\psi-\theta$) for stagnation point flame, S1

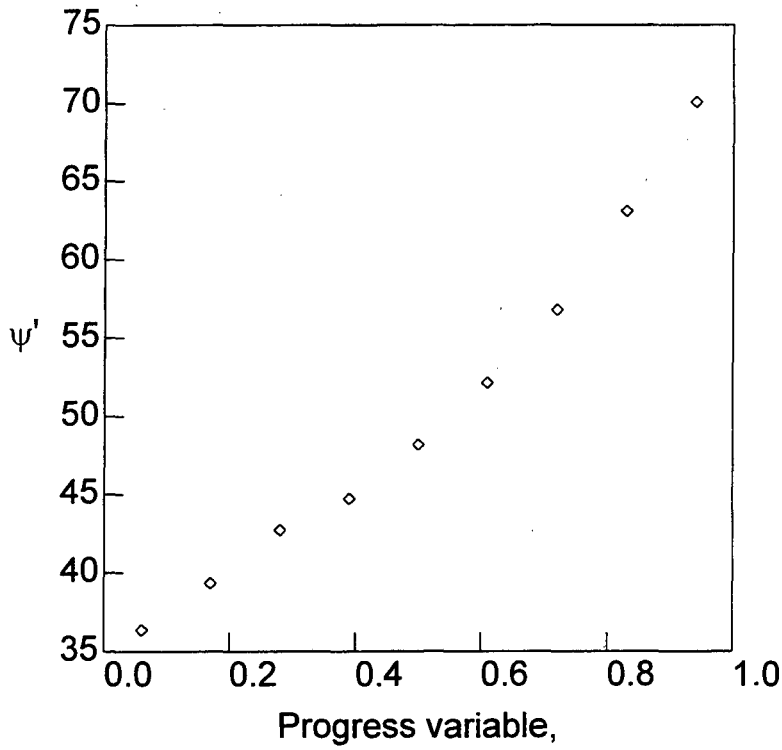

Figure 3 The variation of the flame orientation standard deviation across the flame zone , S1

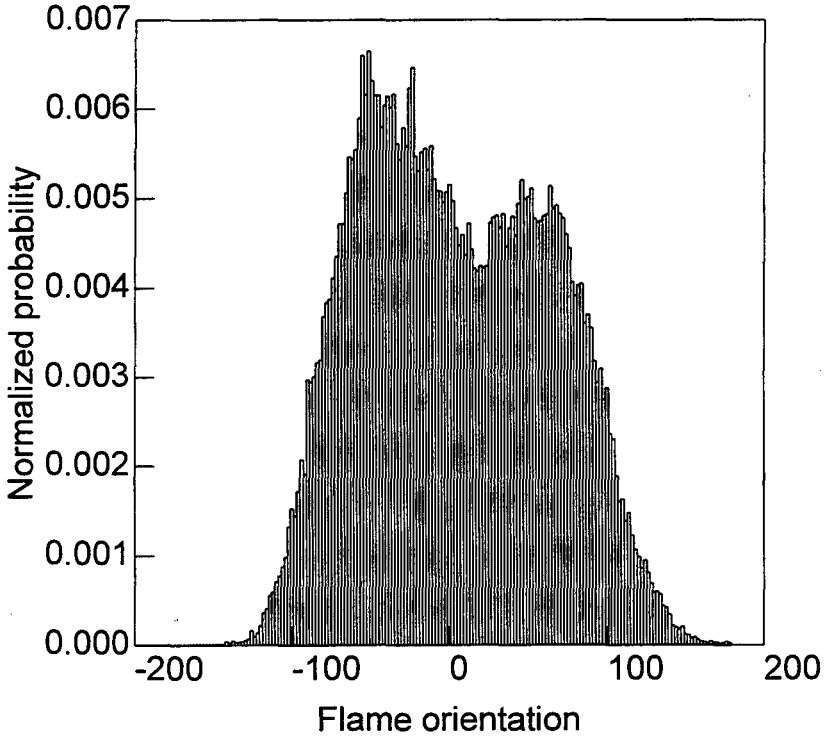

Figure 4 Probability distribution of flame orientation, ($\psi-\theta$) for v-shaped flame

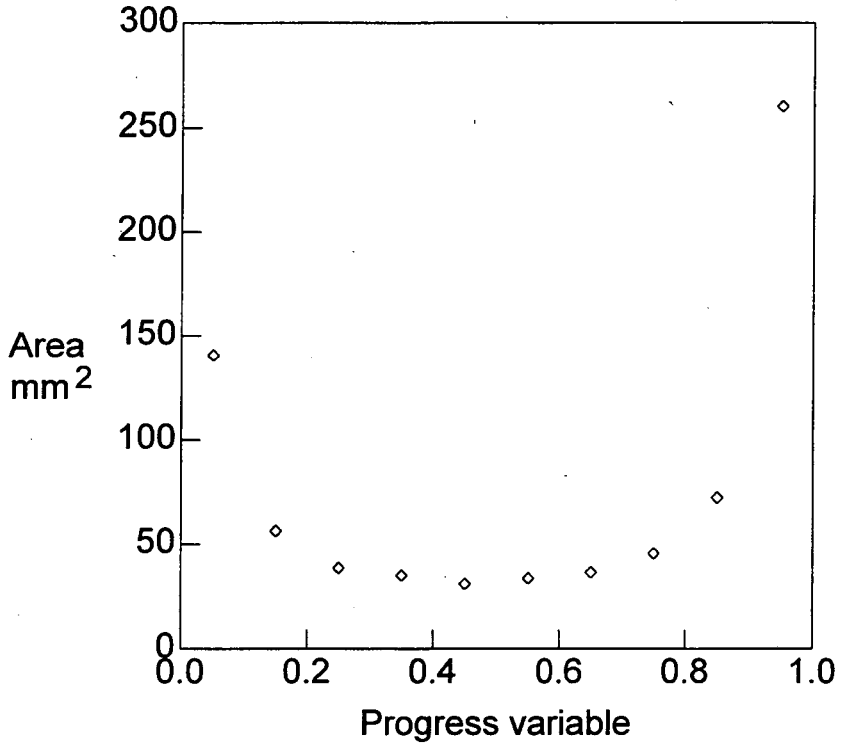

Figure 5 Flame zone area, S1

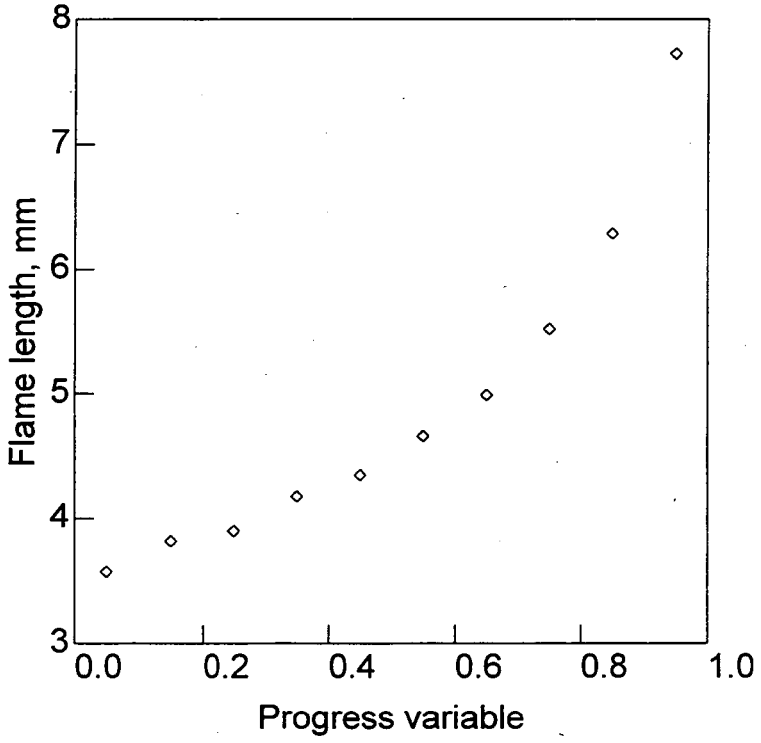

Figure 6 The mean flame length, S1

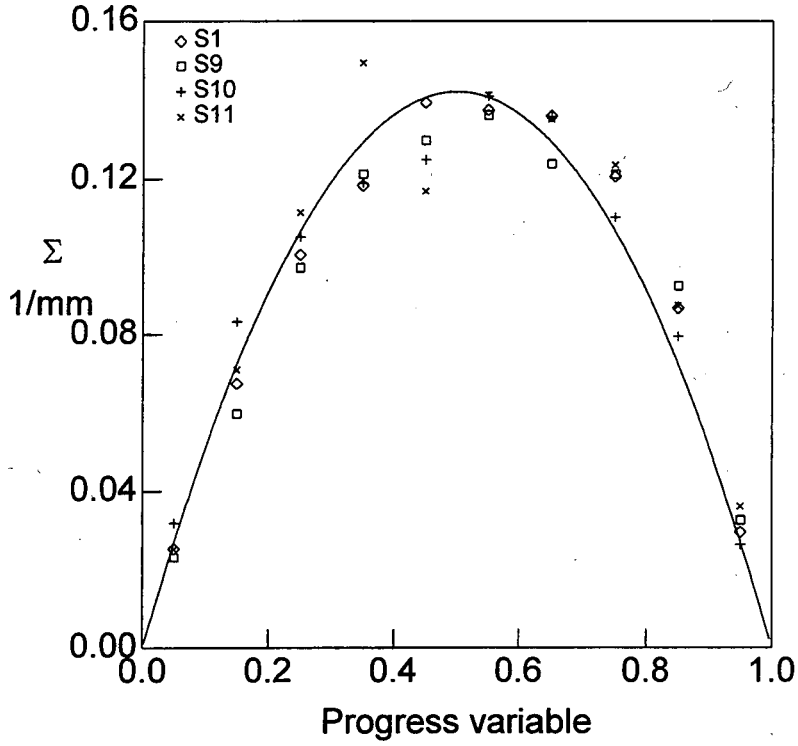

Figure 7 Flame surface density, stagnation point flames.

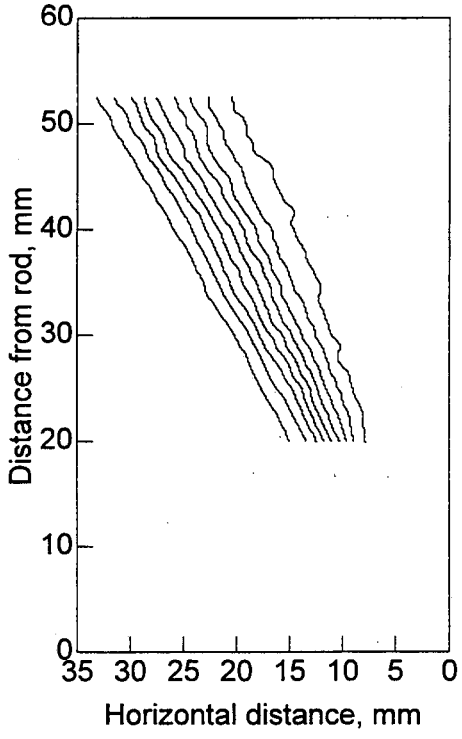

Figure 8 Contours of $\overline{c}$ for v-shaped flame.

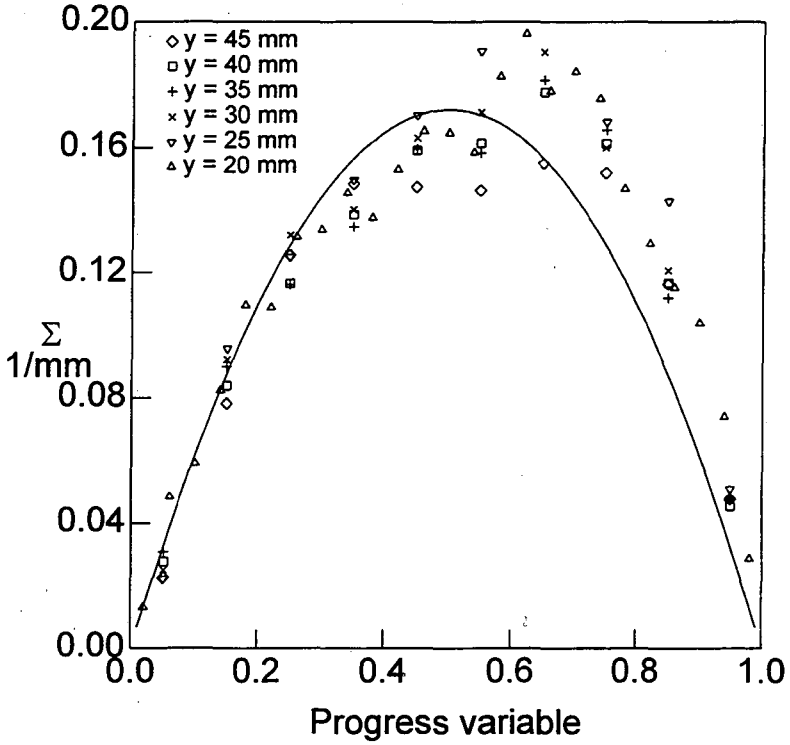

Figure 9 Flame surface density, v-shaped flame.

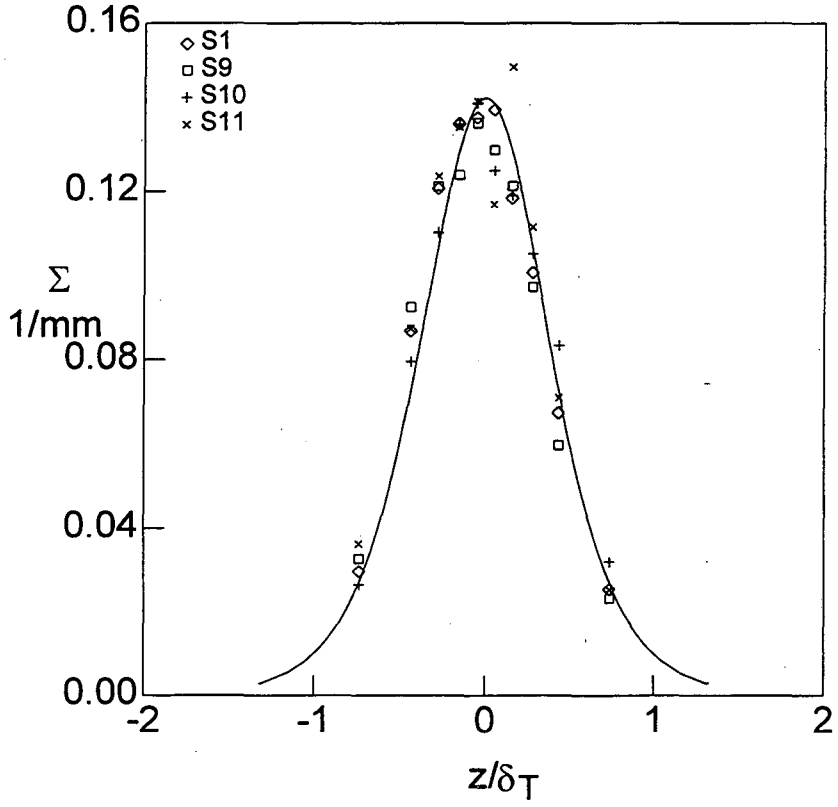

Figure 10 Flame surface density as a function of position in the flame zone, stagnation point flames, z=0 at $\bar{c}$ =0.05.

LAWRENCE BERKELEY LABORATORY
UNIVERSITY OF CALIFORNIA
TECHNICAL AND ELECTRONIC
INFORMATION DEPARTMENT
BERKELEY, CALIFORNIA 94720